Free-stream turbulence effects on the instantaneous pressure and forces on cylinders of rectangular cross section

H. Noda, A. Nakayama

Abstract Simultaneous measurements of instantaneous pressure distributions on rectangular cylinders of length to height ratio(B/D) of 1.0, 2.5 and 3.0 in smooth non-turbulent and homogeneous turbulent flows were made and the data were analyzed by phase averaging and spectral analysis in addition to more conventional methods. The turbulence in the inflow stream is nearly homogeneous and isotropic with the intensity and the scale of 5% and 1.2–1.5 times the cylinder height, respectively. The main effects of the turbulence in the inflow free stream of this scale and intensity are to laterally move the separated shear flow off the upstream corners and cause intermittent reattachment on the side surfaces of cylinders of B/D of 2.5 and larger. For the cylinder with smaller B/D, the flow does not reattach with or without turbulence in the free stream, and the instantaneous surface pressure distributions fluctuate quite periodically at a frequency corresponding to the Strouhal frequency of the vortex shedding. The effects of the free-stream turbulence appear in the increased fluctuation on the front surface as buffeting due to the impinging turbulence. When the separated shear layers reattach due to the influence of the free-stream turbulence, the reattachment point moves intermittently, the pressure distributions downstream of the reattachment fluctuate periodically, and a mild peak is formed in the spectra at a frequency much larger than the Strouhal frequency.

1 Introduction

Recent advances in numerical methods in fluid-flow simulations have made it possible to simulate various turbulent flows including those past bluff bodies. Simulation of turbulent flows when the incident flow is turbulent is very important in engineering applications such as flows past buildings and bridges in natural winds, but has been very difficult. One of the tasks that need to be performed in developing such simulation methods is to verify against known flows, but detailed experimental data on turbulent flow past bluff bodies in turbulent streams are not available at the present time.

More basic experimental investigations, however, have been made to clarify the effects of the free-stream turbulence. Vickery (1966), Roberson et al. (1972), Lee (1975a) and Miyazaki (1980) have investigated the effects of the intensity of the uniform turbulence in the free stream on the drag coefficient and the pressure distribution on a rectangular cylinder. Lee (1975b) and Petty (1979) investigated the effects of the scale of turbulence while Nakamura and Ohya (1984) studied the combined effects of both strength and scale of turbulence and showed that depending on the ratio of the turbulence scale and the cylinder size, the results can be very different. None of these data, however, are meant for detailed validation of simulation methods. Particularly, there are no data for detailed instantaneous forces and pressures on the body together with the detailed characteristics of the free-stream turbulence taken at the same time. The detailed information of the free-stream turbulence will be a prerequisite for serving as a validation test case.

In the present work, we collect detailed data for the turbulence of the oncoming flow including frequency spectra and two-point correlations without the models, and then simultaneous measurements of the instantaneous pressure distributions on all the surfaces of rectangular cylinder models are made. Though only one kind of free-stream turbulence is generated with a turbulence grid, measurements are made on cylinder models of various length-to-height ratios, so that the effects of the free-stream turbulence can be examined in grossly different flow situations.

2 Experimental methods

Experiments were conducted in a large blower-type low-speed wind tunnel with a test section size of 2,000 mm×2,600 mm. A schematic of the setup is shown in Fig. 1. A grid placed 4.2 m upstream of the test model was used to generate free-stream turbulence. The bare wind tunnel without the grid had a turbulence intensity of 0.2%. The cylinder models were supported by the endplates as shown in Fig. 1 in order to ensure two-dimensionality of

Received: 26 October 2000 / Accepted: 11 October 2002
Published online: 1 February 2003

H. Noda
Technical Research Institute,
Mitsui Construction Co. Ltd, Komaki,
270-0132, Nagareyama, Japan

A. Nakayama (✉)
Division of Global Development Science,
Graduate School of Science and Technology,
Kobe University, Rokkodai, Nada-ku, 657-8501, Kobe, Japan
Email: nakayama@kobe-u.ac.jp

本論文は，Experiments in Fluids 34, 2003 より転載したものである。

the flow. The rectangular cylinder models with a cross-section length B to height D ratio of 1.0, 2.5 and 3.0 were tested. It is known that the flow past the rectangular cylinder of aspect ratio B/D=1.0 does not reattach whether or not there is free-stream turbulence. In the case of an aspect ratio larger than about 2.8, the flows separated off the upstream corners of the cylinder reattach even when there is no turbulence in the free stream (Nakaguchi et al.1968), so the results in this range of aspect ratio will contain qualitatively different flows.

The instantaneous surface pressure distribution was measured by PSI pressure transducers, connected to the surface pressure taps via vinyl tubes that allowed simultaneous and fast sampling of fluctuating pressure. The phase lag due to the pressure tubes was compensated using the method of Yoshida et al. (1986). For the cylinders of aspect ratio of 1.0, 2.5 and 3.0, 60, 64 and 72 pressure orifices, respectively, were placed along the center span of the cylinders. In addition to these, 10 orifices were provided in the spanwise direction along the center of all four surfaces of the models. The blockage correction was applied to the instantaneous pressure distributions using the

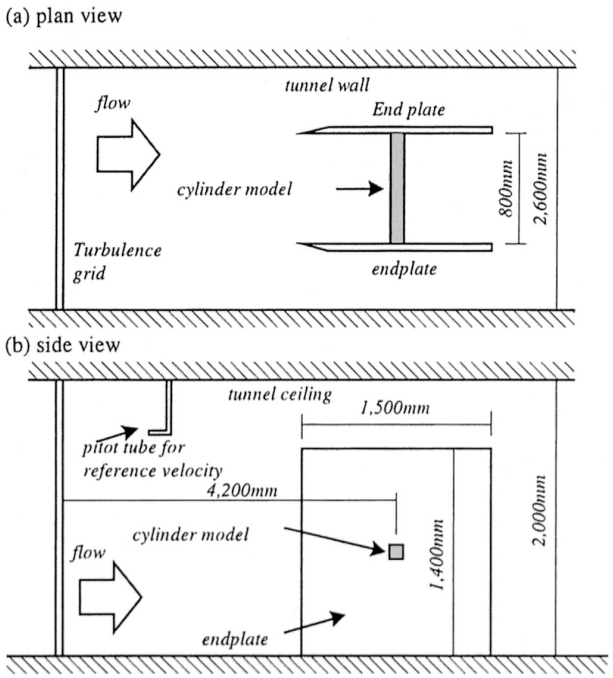

Fig. 1a, b. Experimental setup: **a** plan view; **b** side view

Table 1. Measurement cases and conditions

Case	B/D	Inflow conditions		Re
		Intensity I_n (%)	Scale, L_x	
Case 1	1.0	0.2	–	6.89×10^4
Case 2		5.3	1.13D	
Case 3	2.5	0.2	–	5.16×10^4
Case 4		5.3	1.50D	
Case 5	3.0	0.2	–	5.16×10^4
Case 6		5.3	1.50D	

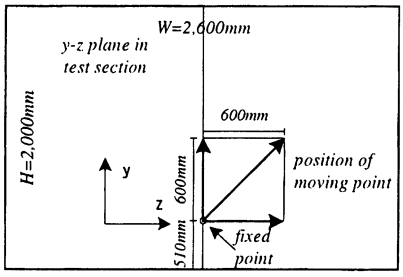

Fig. 2. Measurement point

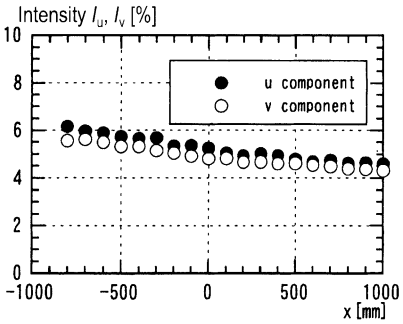

Fig. 3. Turbulence intensities along centerline of tunnel

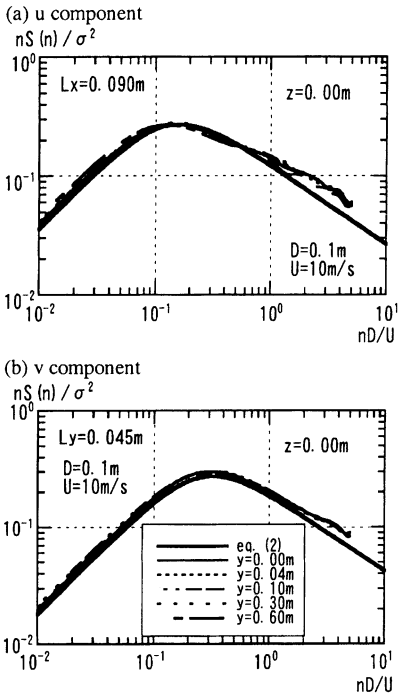

Fig. 4a, b. Power spectral density of fluctuating velocity components: **a** u component; **b** v component

本論文は，Experiments in Fluids 34, 2003 より転載したものである。

method of Nakamura and Ohya (1984), which was originally used to correct the average pressures. The measurements were made at the tunnel speed U_{ref} of approximately 13 m/s so that the Reynolds number based on U_{ref} and the height of the cylinders, D was 6.89×10^4 for the cylinder with B/D=1.0, in which case D=80 mm, and 5.16×10^4 for the cylinders of B/D=2.5 and 3.0, in which cases D=60 mm. The measurement cases are summarized in Table 1.

Statistics of the fluctuating velocity components in the free stream were measured using a set of two X-wire hot wire probes in order to quantify the detailed characteristics of the turbulence. One of the probes was fixed in space and the other was translated along the cross-stream, spanwise and the diagonal directions, as shown in Fig. 2, at varying distances from the fixed one in order to obtain two-point statistics. In the following, x is the coordinate in the main flow direction, y is the coordinate in the normal direction, and z is the spanwise coordinate. The instantaneous velocity components in these directions are denoted by u, v, and w, respectively.

3 Experimental results

3.1 Results of characteristics of free-stream turbulence

First we describe the results of the detailed turbulence measurements in the flow without the models. The distributions of the relative turbulence intensities of streamwise fluctuation I_u and vertical fluctuation I_v, defined by

$$I_u = \frac{\sqrt{\overline{u_i'^2}}}{U_i},\quad I_v = \frac{\sqrt{\overline{v_i'^2}}}{U_i}, \tag{1}$$

where u_i and v_i are the fluctuating velocity components, and U_i is the mean velocity at point i, along the wind tunnel axis, are shown in Fig. 3. It is seen that both intensities slowly decay from about 6% 800 mm upstream to about 4% 1,000 mm downstream of the position where the models are to be positioned. Streamwise intensity I_u is 5.3% and the normal intensity I_v is 4.8% at the model positions, and they indicate slight deviation from isotropy.

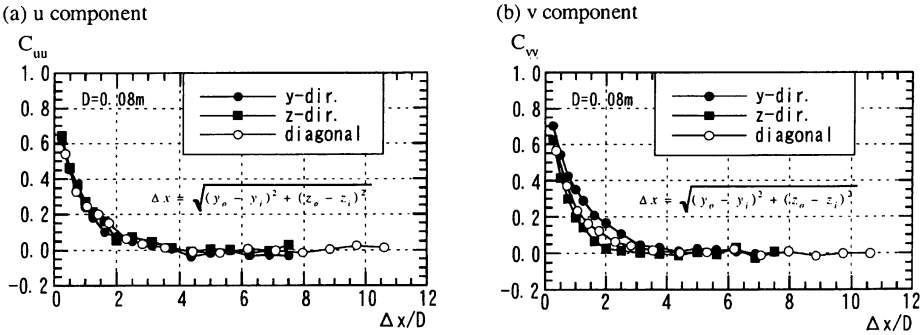

Fig. 5a, b. Two-point correlation coefficients of fluctuating velocity components: **a** u component; **b** v component

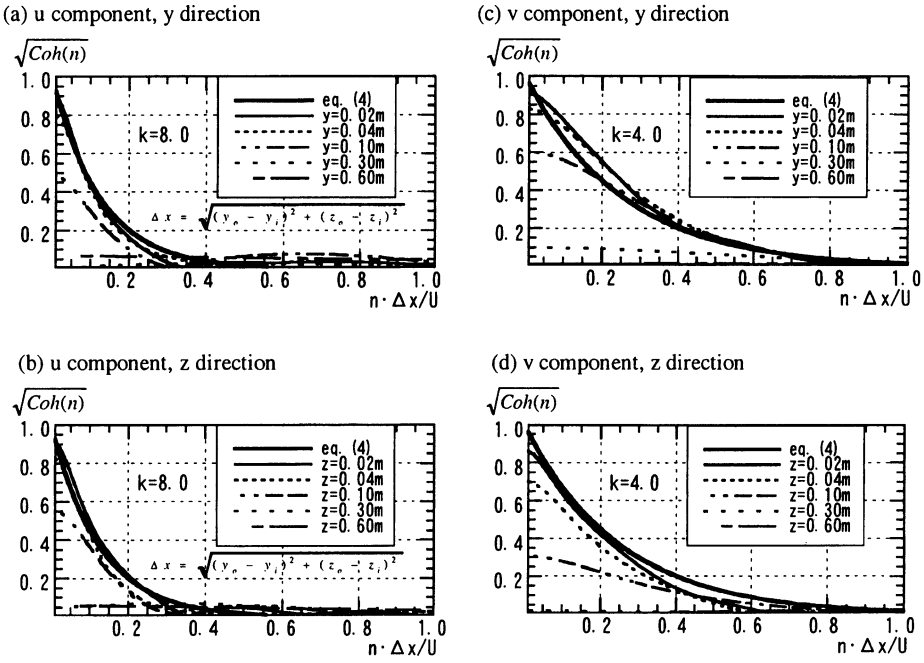

Fig. 6a–d. Root coherence of fluctuating velocity components: **a** u component, y direction; **b** u component, z direction; **c** v component, y direction; d v component, z direction

本論文は，Experiments in Fluids 34, 2003 より転載したものである。

The power spectra S of u and v at several vertical positions in the center span at the model location are shown in Fig. 4. The Kármán spectrum,

$$S_i(n) = \frac{4\sigma^2 L_x/U_i}{\left[1+70.8(nL_x/U_i)^2\right]^{5/6}}, \quad (2)$$

where σ is the rms fluctuation of either u or v velocity component, L_x is the integral scale, and n is the frequency, is also shown for comparison. The measured spectra are seen to be very close to the Kármán spectrum except in the high-frequency range, where the measured ones are slightly higher. The integral length scales from these spectra have been determined and found to be 0.090 m from the u spectra and 0.045 m from the v spectra. The ratio is 2 in the case of isotropic turbulence, and the present values of the integral scales satisfy this relation.

The two-point velocity correlation coefficients defined by

$$C_{uu} = \frac{\overline{u'_o u'_i}}{\sqrt{\overline{u'^2_o}}\sqrt{\overline{u'^2_i}}}, \quad C_{vv} = \frac{\overline{v'_o v'_i}}{\sqrt{\overline{v'^2_o}}\sqrt{\overline{v'^2_i}}}, \quad (3)$$

where u'_o and v'_o are the fluctuating streamwise and normal velocity components at the fixed point, and u'_i and v'_i are the fluctuating streamwise and normal velocity components at the moving point separated by $\Delta x = \sqrt{(y_i - y_o)^2 + (z_i - z_o)^2}$ from the fixed position. The results for the three directions of the separation vectors are shown in Fig. 5. The three two-point correlations of u shown here are all transverse correlations because the direction of the flow is perpendicular to the vector in the direction of the separation between the fixed and moving point, and should be the same if the turbulence was isotropic

Table 2. Aerodynamic characteristics obtained by present measurement and previous studies

	Inflow conditions		*Re*	*St*	C_{pb}	C_D	C'_D	C'_L
	Intensity(%)	Scale						
(a) *B*/*D*=I.0								
Present	0.2	–	6.89×10^4	0.131	−1.483	2.164	0.207	1.180
	5.3	1.12D	0.133	−1318	1.989	0.203	1.105	
Nakaguchi et al. (1968)	Smooth	–	$2\sim6\times10^4$	0.13	−1.50	2.10	–	–
Ootsuki et al. (1980)	0.2	–	$6.5\sim7\times10^4$	0.12	−1.35	2.08	0.11	0.82
Bearman and Trueman (1972)	Smooth	–	6.8×10^4	0.13	−1.40	2.19	–	–
Bearman and Obasaju (1982)	Smooth	–	4.7×10^4	0.125	−1.65	–	–	–
Mizota and Okajima(1982)	Smooth	–	7.14×10^4	0.125	−1.64	–	–	–
Okajima (1982)	Smooth	–	4.2×10^4	0.13	−1.47	–	–	–
Durao et al. (1988)	6	–	1.4×10^4	0.138	–	–	–	–
Lyn and Rodi (1994)	2	–	2.2×10^4	0.132	–	–	–	–
Vickery (1966)	Smooth	–	1.0×10^5	0.118	−1.31	–	–	–
	10.0	1.33D	–	0.120	−0.71	–	–	–
Roberson et al. (1972)	0.5	–	2.16×10^4	–	−1.13	1.19	–	–
	4.0	–	1.97×10^4	–	−1.06	1.85	–	–
	8	–	2.02×10^4	–	−0.88	1.65	–	–
Lee (1975a)	0.5	–	1.76×10^4	0.122	−1.30	2.05	–	–
	6.5	–	1.14D	0.126	−1.18	1.93	–	–
Petty (1979)	Smooth	–	2.9×10^4	–	−137	–	–	–
	4.0	0.9D		–	−1.19	–	–	–
	8.0	1.1D		–	−0.96	–	–	–
Nakamura and Ohya (1984)	0.12	–	6.6×10^4	–	−1.50	–	–	–
	6.1	0.85D		–	−1.20	–	–	–
	10.0	1.05D		–	−0.97	–	–	–
Tamura and Miyagi (1998)	0.4	–	3.0×10^4	–	–	2.09	–	1.05
	6.5	0.76D		–	–	1.79	–	0.74
	14.0	0.80D		–	–	1.49	–	0.34
(b) *B*/*D*=2.5								
Present	0.2	–	5.16×10^4	0.070	−0.746	1.562	0.054	0.256
	5.3	1.5D		0.049, 0.169	−0.558	1.346	0.119	0.217
Nakaguchi et al. (1968)	Smooth	–	$2\sim6\times10^4$	0.07	−0.62	1.32	–	–
Ootsuki et al. (1980)	0.2	–	$6.5\sim7.6\times10^4$	0.06	−0.46	1.42	0.03	0.28
Okajima (1982)	Smooth	–	4.2×10^4	0.06, 0.12	−0.53	–	–	–
(c) *B*/*D*=3.0								
Present	0.2	–	5.16×10^4	0.163, 0.049	−0.641	1.472	0.070	0.137
	5.3	1.5D		0.168, 0.051	0.487	1.312	0.110	0.152
Nakaguchi et al. (1968)	Smooth	–	$2\sim6\times10^4$	0.154	−0.50	1.23	–	–
Ootsuki (1980)	0.2	–	$6.5\sim7.6\times10^4$	–	−0.35	1.26	0.05	0.31
Okajima (1982)	Smooth	–	4.2×10^4	0.15	−0.44	–	–	–

本論文は，Experiments in Fluids 34, 2003 より転載したものである。

and the measured results indicate this fairly accurately. The correlation between v'_o and v'_i separated in the y direction is the longitudinal correlation and should be the largest, which is what is seen in the plot. C_{vv} with separation vector aligned in the z direction is the transverse correlation, and if isotropic, should be close to C_{uu} shown in Fig. 4a. C_{vv}, however, appears to be slightly lower than C_{uu}.

The root coherence of two velocities, either u or v at two points is defined by

$$\sqrt{Coh}(n) = \frac{|S_{oi}|}{\sqrt{S_o}\sqrt{S_i}}, \tag{4}$$

where S_{oi} is the cross spectrum between the fluctuating velocities at the fixed point and the moving point, and S_o and S_i are the spectral densities of the fluctuating velocity at the fixed point and at the moving point, respectively, and n is the frequency. The measured results for the root coherence along with the approximate formula due to Davenport

$$\sqrt{Coh}(n) = \exp\left\{\frac{-kn\Delta x}{U}\right\} \tag{5}$$

are shown in Fig. 6. k in this approximation is the correlation coefficient, and the values of k=8 and 4 are recommended for u and v coherences, respectively. It is seen that the root coherence for u can be approximated fairly well by Eq. (5) with k=8, when there is no separation in the y and z directions. This is the limitation of Eq. (5), which does not consider separation in the y and z directions. The root coherence for v is seen to behave about the same way

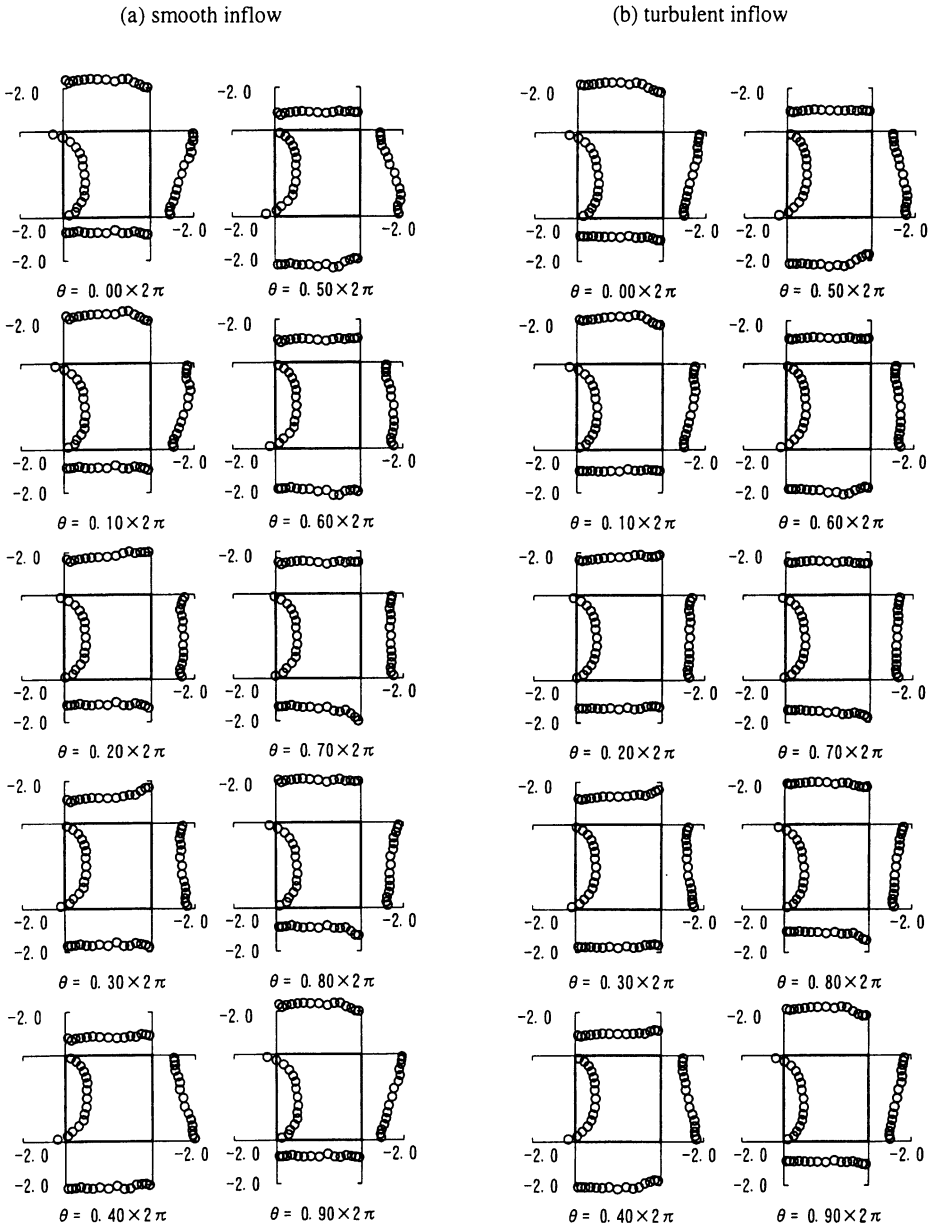

Fig. 7a, b. Phase-averaged surface pressure distribution, B/D=1.0: **a** smooth inflow; **b** turbulent inflow

as that for u, but the values are considerably larger and over a larger frequency range.

3.2
Drag and lift coefficients

The mean drag coefficient and the rms fluctuation of the instantaneous drag and lift coefficients defined by

$$\bar{C}_D = \frac{\bar{f}_D}{\frac{1}{2}\rho U_{ref}^2},\ C'_D = \frac{f'_D}{\frac{1}{2}\rho U_{ref}^2},\ C'_L = \frac{f'_L}{\frac{1}{2}\rho U_{ref}^2}, \quad (6)$$

where $\bar{f}_D$ is the mean drag force and f'_D and f'_L are the fluctuating drag and lift forces, respectively and U_{ref} is the velocity at the upstream reference position together with the base-pressure coefficient C_{pb} and the Strouhal number St, as determined from spectral analysis of fluctuating pressure, are summarized in Table2. The results obtained without the turbulence grid, in which case the tunnel turbulence intensity is 0.2% and designated as the "smooth" flow, are also shown. Also the existing data obtained by other authors are included for comparison wherever possible. The present results agree with the other data in general. The mean drag coefficient is seen to decrease due to the free-stream turbulence for all aspect ratios, while the fluctuating drag increases. The effects on the fluctuating lift coefficients are to reduce in the case of B/D=2.5 but increase for the fully reattaching flow case of B/D=3.0. They seem to have little effect for the fully separated case of B/D=1.0.

3.3
Instantaneous and phase-averaged surface pressure distributions

The instantaneous surface-pressure distributions at consecutive times at an interval of 0.005 s were analyzed to examine the features of the fluctuations. For the cases with clear vortex-shedding type flow unsteadiness, the pressure

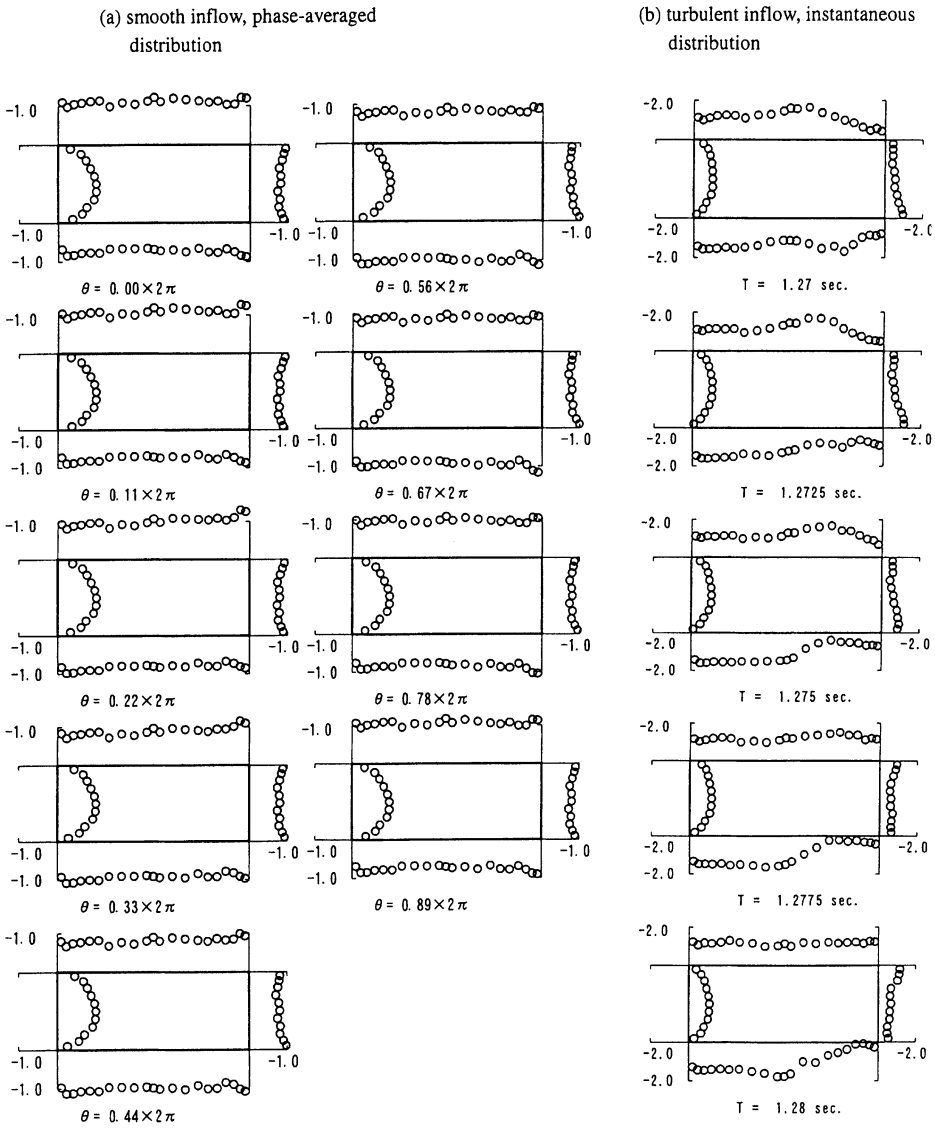

Fig. 8. a Smooth inflow, phase-averaged surface pressure distribution; **b** turbulent inflow, instantaneous surface pressure distribution, B/D=2.5

本論文は，Experiments in Fluids 34, 2003 より転載したものである。

near the upstream corners on the front surface exhibited clear periodic changes, which was used to identify the phase of the vortex-shedding cycle. For these cases, the phase-averaged surface pressure fluctuations are examined. Figure 7 shows the phase-averaged surface pressure distributions for the case of B/D=1.0, which showed a clear vortex shedding. θ is the phase angle in radian. In the case of B/D=2.5, discernible periodicity was observed for the case of smooth inflow, but for the turbulent inflow, the vortex shedding was not strong enough to show periodicity in the phase-detecting pressure on the front surface. So in Fig. 8 the phase-averaged pressure distributions are shown for the smooth flow only, and the instantaneous distributions are shown for the turbulent flow. For B/D=3.0, no periodicity was observed for both smooth and turbulent inflow cases and instantaneous distributions are shown in Fig. 9. The pressures are shown in terms of the pressure coefficient defined by

$$C_{\mathrm{p}} = \frac{p_i - p_{\mathrm{ref}}}{\frac{1}{2}\rho U_{\mathrm{ref}}^2} \tag{7}$$

where p_{ref} is the static pressure at the reference position.

It can be seen in Fig. 7 that, in the case of B/D=1.0, the results for the smooth flow and turbulent flow are about the same, and the pressures on all surfaces fluctuate at a frequency corresponding to that of the vortex shedding and the distribution is anti-symmetric about the centerline of the model. The amplitude of fluctuation decreases slightly towards the downstream end of the side surface where a slight phase lag is also seen.

The smooth-flow results for the case of B/D=2.5 shown in Fig. 8 show fewer periodic fluctuations compared with the case of B/D=1.0, but a weak periodic fluctuation is seen in the side-surface pressure distributions. The turbulent

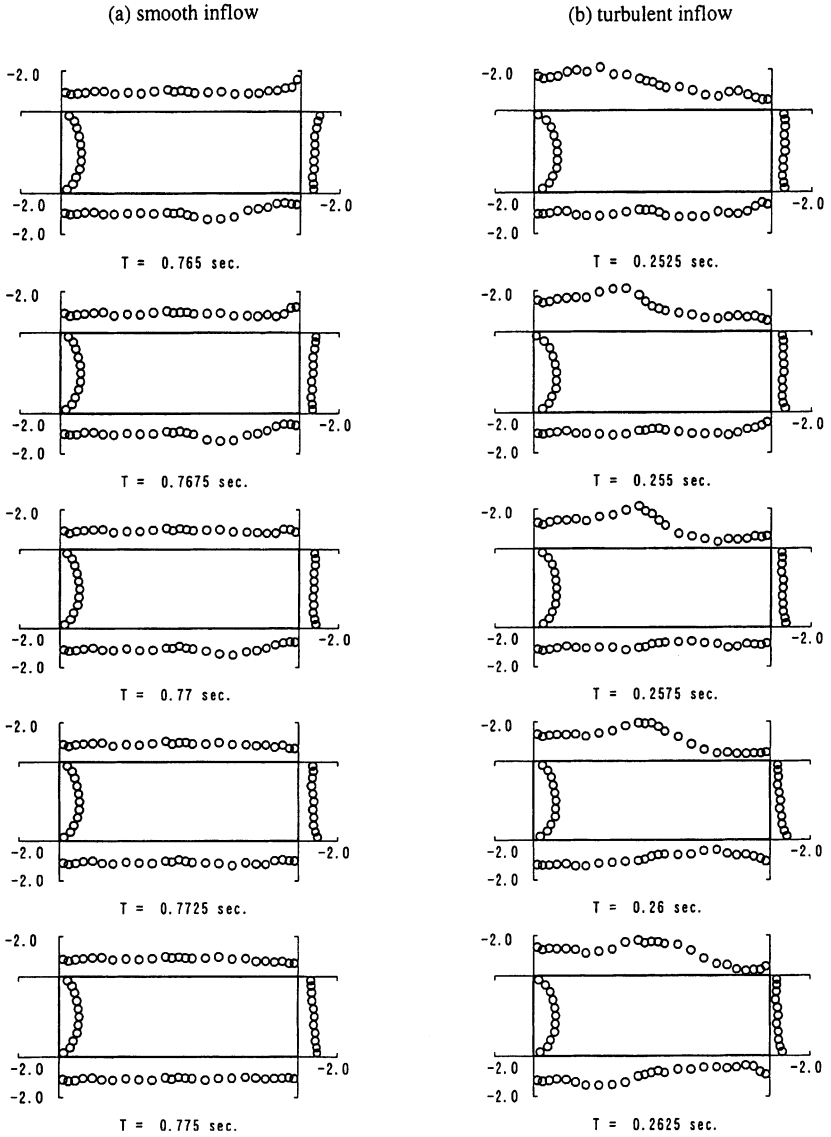

Fig. 9a, b. Instantaneous surface pressure distribution, B/D=3.0: **a** smooth inflow; **b** turbulent inflow

本論文は，Experiments in Fluids 34, 2003 より転載したものである。

inflow case shown in Fig. 8b shows large wavy fluctuations over the downstream half of the side surfaces, though not on the fixed-phase basis, and the waviness is seen to propagate in the downstream direction. This is considered to be due to an unsteady reattachment of the flow separated at the upstream corners. When the reattachment occurs, the fast flow reaches the surface and creates negative peaks in the surface pressure distribution. As the aspect ratio is increased to B/D=3.0, clear periodicity is lost for both smooth and turbulent inflow cases and instantaneous distributions are shown. The overall fluctuations are small when the inflow is smooth and the reattachment occurs more steadily compared with the turbulent inflow case of B/D=2.5. When the inflow is turbulent, the pressure over the downstream half of the side surfaces change with large amplitude and is very much like the case of B/D=2.5, with distinct negative peaks traveling downstream. These results indicate that the turbulence in the free stream causes flapping of the separated shear flow and, for cylinders of B/D=2.5 or larger, it is made to reattach intermittently on the side surface. This causes a fluctuation of the surface pressure near the downstream end of the cylinder. The case of B/D=2.5 is the critical case, in which the flow does not reattach without the free-stream turbulence, but with the turbulence unsteady reattachment occurs.

3.4
Mean and rms pressure coefficients

The mean pressure coefficient and the rms pressure fluctuations defined by

$$\overline{C_p} = \frac{\overline{p_i - p_{ref}}}{\frac{1}{2}\rho U_{ref}^2},\quad C_p' = \frac{\sqrt{\overline{(p_i - \bar{p}_i)^2}}}{\frac{1}{2}\rho U_{ref}^2} \tag{8}$$

are plotted in Figs. 10 and 11. In the case of B/D=1.0, the results for both smooth and turbulent flows are about the same except that a slightly higher pressure recovery is seen on the rear surface. In the case of B/D=2.5 and 3.0, the mean pressure on the side surfaces stay about constant in the smooth flow, while it rises rapidly downstream of the mid chord in the turbulent flow. For the larger B/D of 3.0, the recovery distance is longer, and the amount of recovery is also larger. Nakamura and Ohya (1984) showed that, in the case of completely separated flow, the free-stream turbulence with small length scale ($L_x \approx 0.1D$) enhances the entrainment of the separated shear flow and that with scale comparable to D weakens the vortex shedding. The scale of the present free-stream turbulence is 1.2D in the case of B/D=1.0 and 1.5D for B/D=2.5 and 3.0, which means that the scale is comparable to the cylinder size but the spanwise correlation shown below does not necessarily indicate weakening.

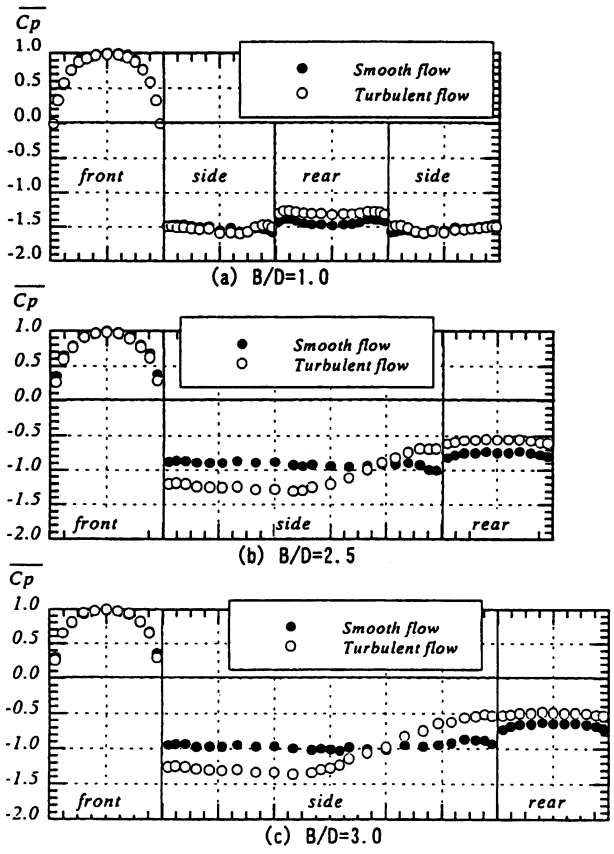

Fig. 10. Mean pressure coefficient

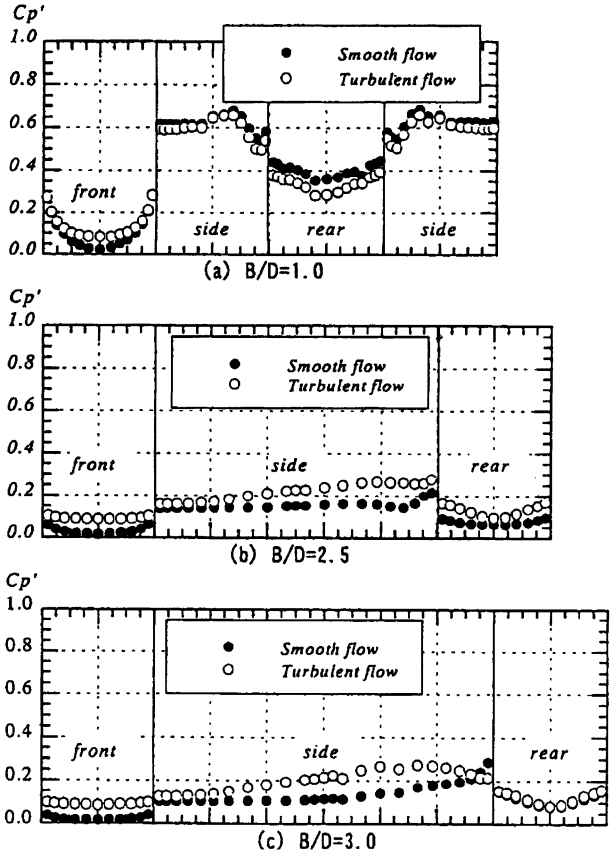

Fig. 11. Rms pressure fluctuation

Next, the pressure fluctuation intensity results are examined. In the case of B/D=1.0, the pressure fluctuation on the front surface in the smooth flow case is very small at the center and increases towards the corners while, in the cases of B/D=2.5 and 3.0, it is small across the entire front surface. This is perhaps related to the fluctuation level on the side surfaces, which is very large for the fully separated case of B/D=1.0 compared with the reattaching cases of B/D=2.5 and 3.0. In turbulent inflow cases of B/D=2.5 and 3.0, the fluctuation level reaches maximum near x/D=2.0. According to Ishizaki and Katsura (1974), the pressure fluctuation level becomes maximum near the reattachment point and the reattachment in the present flow is considered to occur near x/D=2.0. In the case of smooth inflow of

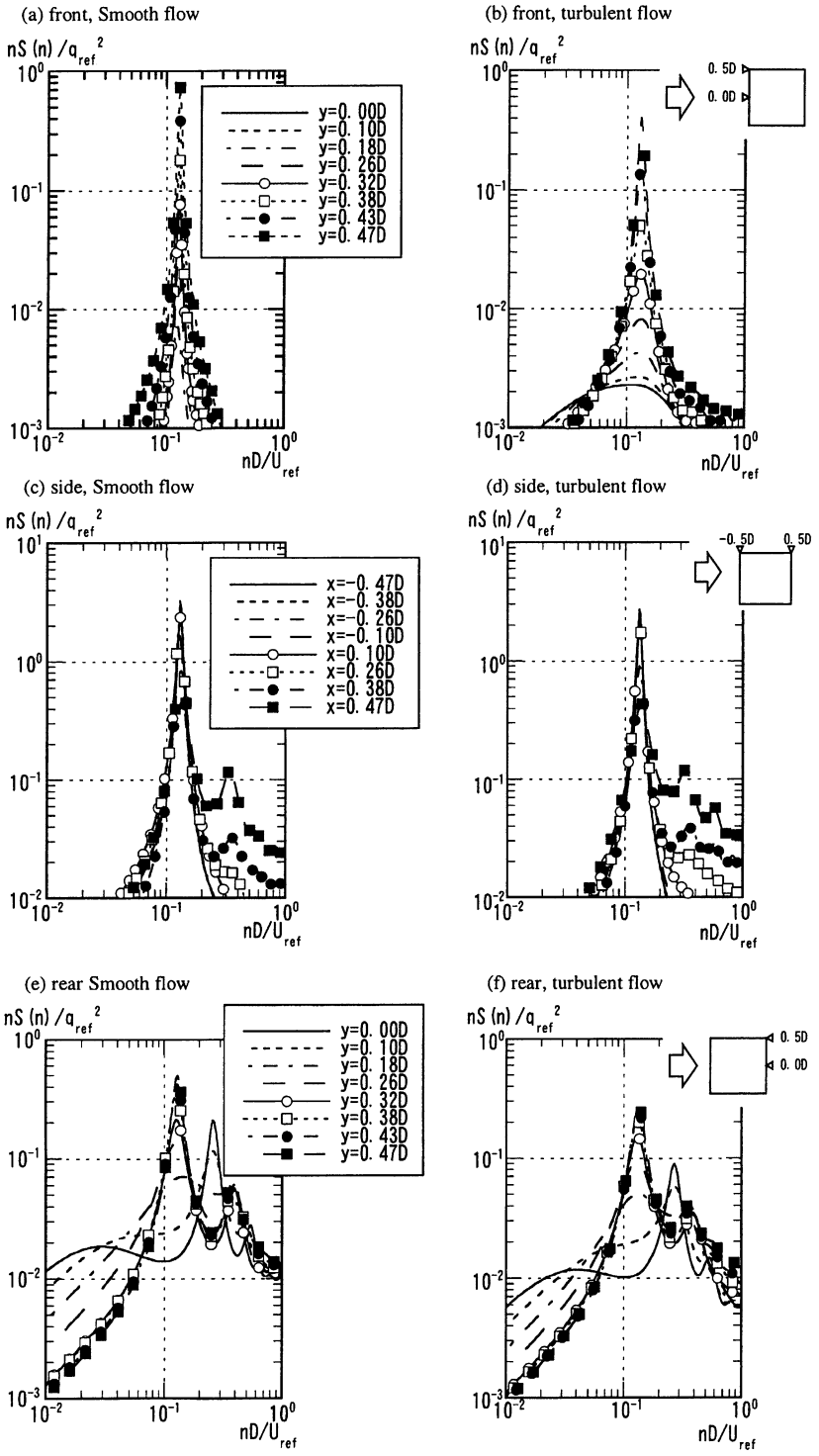

Fig. 12a–f. Power spectral density of fluctuating pressure, B/D=1.0: **a** front, smooth flow; **b** front, turbulent flow; **c** side, smooth flow; **d** side, turbulent flow; **e** rear, smooth flow ; **f** rear, turbulent flow

B/D=2.5, no clear local maximum is seen and is an indication of no reattachment.

3.5
Power spectral density of fluctuating surface pressure

The power spectral density of the fluctuating pressure on the three surfaces of the model for the cases with and without the free-stream fluctuation are shown in Figs. 12, 13 and 14 for B/D=1.0, 2.5 and 3.0, respectively. The ordinate is normalized by the square of the dynamic pressure q_{ref} at the reference position.

In the case of B/D=1.0, the flow is fully separated irrespective of the existence of the free-stream turbulence. The spectra on all surfaces shown in Fig. 12 for both smooth and turbulent-flow cases contain strong peaks corresponding to the Strouhal frequency of the vortex shedding. The only difference between the smooth and turbulent cases is seen near the center (y/D=0) of the front surface, where the spectra for the turbulent inflow case look closer to the spectra of the inflow turbulence shown in Fig. 4. Therefore, the free-stream turbulence in the fully separated case merely causes a buffeting by the impinging turbulence. The spectra on the side surfaces are little influenced by the free-stream turbulence, and both cases show higher frequency contributions as the downstream corner is approached. These are smaller peaks at approximately twice the Strouhal frequency and perhaps related higher modes. The spectra on the rear surface contain both the high-frequency contributions and additional lower-frequency contributions near the center of the surface. These low-frequency contributions near the

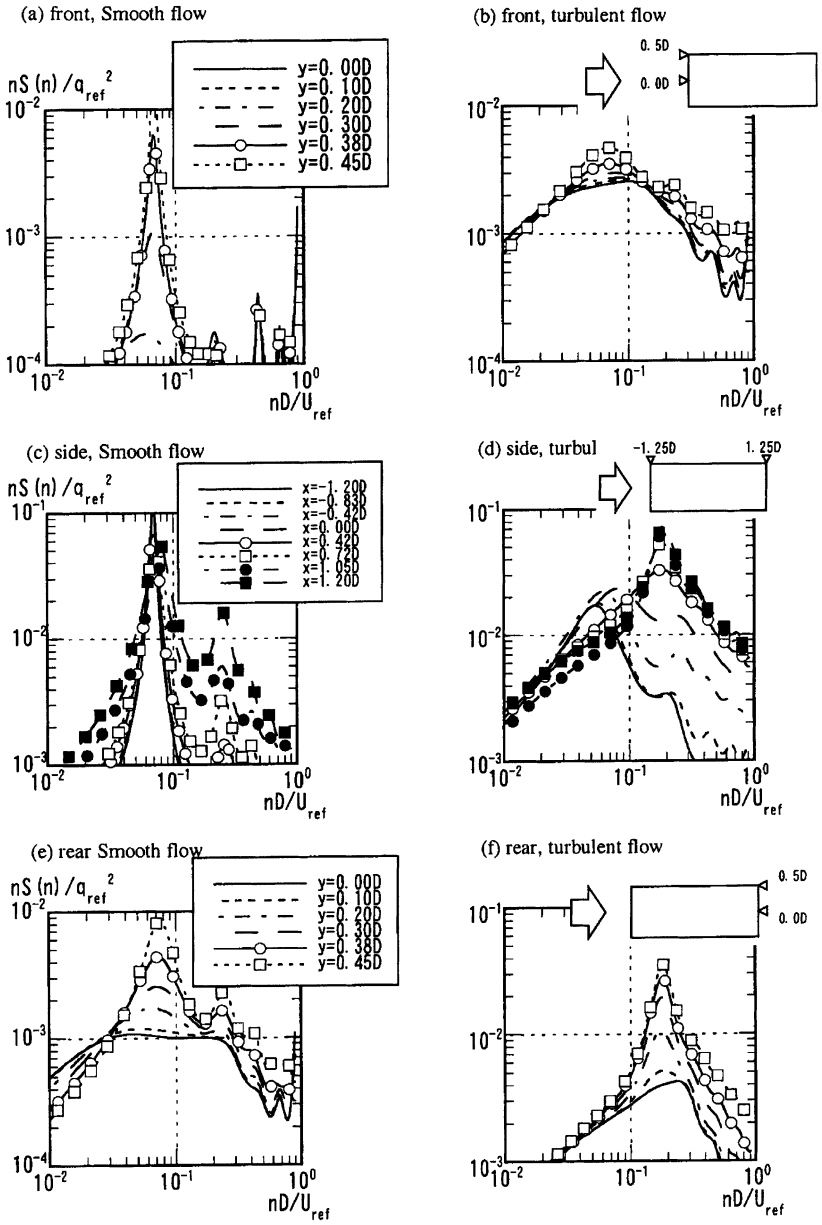

Fig. 13a–f. Power spectral density of fluctuating pressure, B/D=2.5: **a** front, smooth flow; **b** front, turbulent flow; **c** side, smooth flow; **d** side, turbulent flow; **e** rear, smooth flow ; **f** rear, turbulent flow

本論文は，Experiments in Fluids 34, 2003 より転載したものである。

center of the body are considered to be due to the slow oscillation of the recirculating flow just downstream of the body.

In the case of B/D=2.5, the spectra of the fluctuating pressure are very different between the smooth and turbulent inflow cases. The smooth-flow results show peaks near nD/U_{ref}=0.07 that are considered to be due to the vortex shedding, since they are seen on all surfaces except near the center of the rear surface. This low frequency of vortex shedding also agrees with the previous results of Nakaguchi et al. (1968). The peak values are significantly smaller, indicating weaker shedding. The spectra for the turbulent inflow case look very different. Those on the front surface are very close to those of the inflow turbulence, except near the corner (y/D=0.5), where very gentle peaks are seen that correspond to the Strouhal frequency of the smooth-flow case (nD/U_{ref}=0.07). These small peaks, which may be related to the premature vortex shedding that may be starting near the corners, diminish at downstream positions of the side surfaces and disappear altogether at the downstream corner. Here, broad high-frequency contributions due to turbulent fluctuations dominate.

In the case of B/D=3.0, the spectra of pressure on the front surface of even the smooth inflow case do not show distinct peaks. This is consistent with the data of the instantaneous pressure distributions. The spectra of the turbulent inflow case are now almost exactly the same as the inflow turbulence. On the side surfaces, peaks that are not very clear appear at about nD/U_{ref}=0.17 for both cases, and they grow as the downstream corner is approached. Contributions from other frequencies over wider range also grow. On the rear surface, the direct effects of the inflow turbulence are not seen, and the results for both smooth and turbulent inflow cases are almost the same, except the turbulent inflow case shows larger contributions from the high-frequency fluctuations.

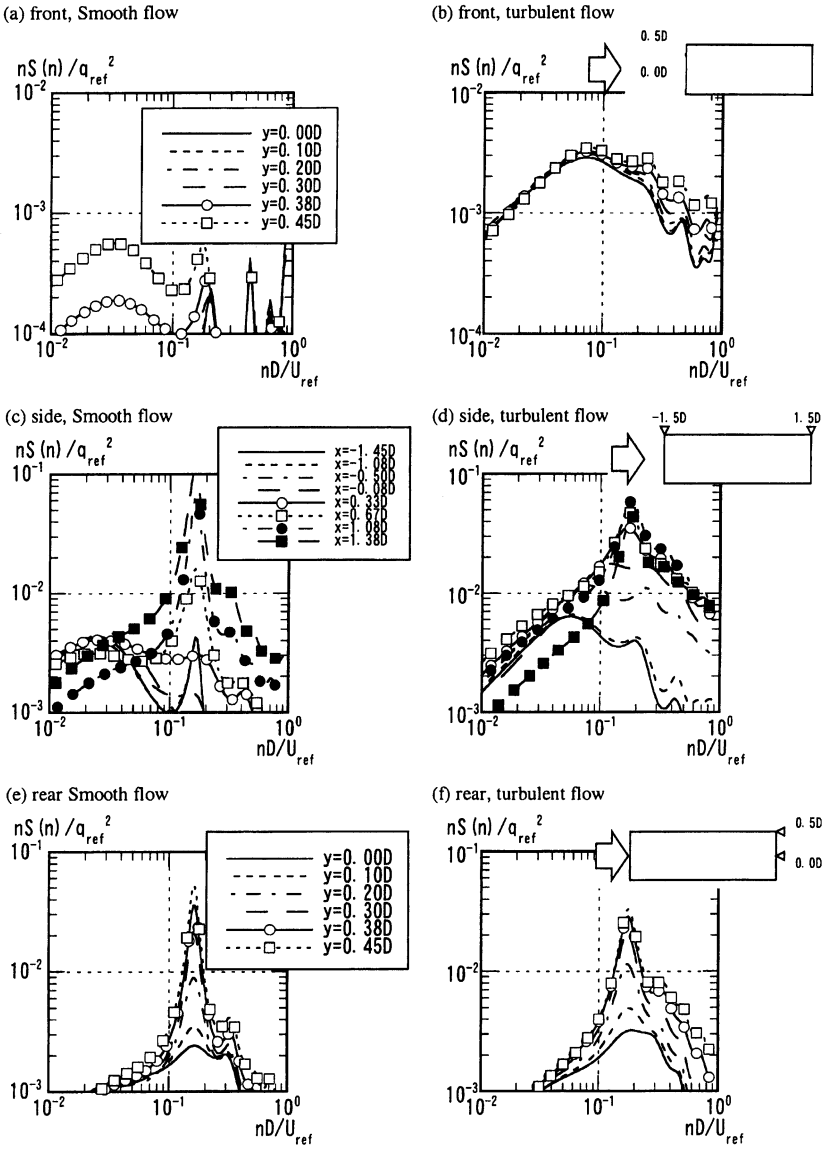

Fig. 14. Power spectral density of fluctuating pressure, B/D=3.0

3.6
Spanwise correlation of surface pressure

In order to study the effects of the free-stream turbulence on the spanwise structure, the spanwise pressure correlation coefficient defined by

$$C_{pp} = \frac{\overline{p'_o p'_i}}{\sqrt{\overline{p'^2_o}}\sqrt{\overline{p'^2_i}}} \qquad (9)$$

where p'_o and p'_i are the fluctuating pressures at the fixed and point i, was obtained and plotted in Fig. 15.

In the case of B/D=1.0, the correlation of the pressure on the side surfaces is reduced slightly due to the turbulent flow. This is in agreement with Nakamura and Ohya's (1984) results. The correlation on the rear surface, on the other hand, is larger. In the cases of B/D=2.5 and 3.0, the high correlations on the side surfaces in the smooth flow are significantly reduced by the turbulent flow. The effects on the correlation on the rear surface are similar to the case of B/D=1.0 and it is larger in the turbulent flow. The main reason for the reduced correlation on the side surface by the free-stream turbulence is considered to be the shift of the reattachment position and its intermittent nature. The fact that the spanwise correlation of the pressures on the rear surface is increased by the free-stream turbulence is due to the increased turbulence downstream of reattachment and in the near wake tending to equalize the correlations on both surfaces.

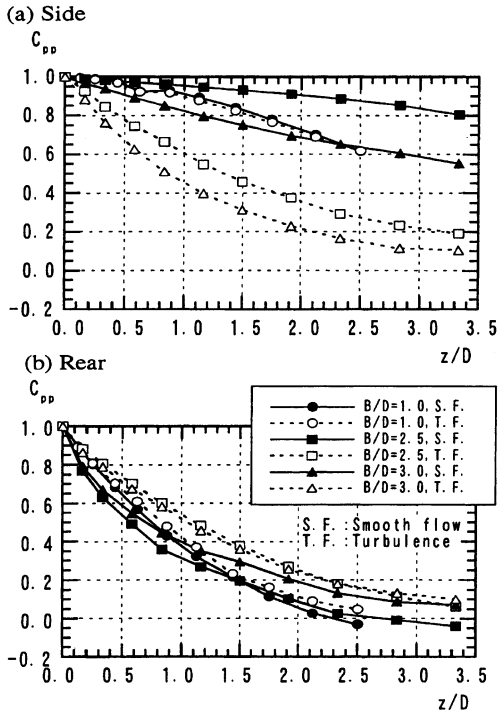

Fig. 15a, b. Spanwise correlation of surface pressure: **a** side; **b** rear

4
Discussion

While the data presented in the present paper are mainly for documentation of the properties of the fluctuating surface-pressure distributions and the resulting aerodynamic forces, the simultaneously sampled instantaneous pressure distributions together with their spectral analysis allow us to clarify some of the flow physics important to the effects of the free-stream turbulence. It is known that the free-stream turbulence promotes reattachment and changes the overall flow characteristics, but how the instantaneous flow is influenced by the turbulence in the free stream has not been clear. The present data indicate that, when the length to height ratio B/D of the rectangular cross section is either as small as 1.0 or as large as 3.0, the turbulence in the inflow does not alter the overall characteristics of the fluctuation of the flow and the surface pressure. The main effects occur when B/D is in the critical range near B/D=2.5, which corresponds to the range where Nakaguchi et al. (1968) found a sudden change in the vortex shedding characteristics when there is no free-stream turbulence. The way the turbulence in the inflow influences the flow may be summarized as follows. The turbulence with the length scale of the same order as D, which is the scale in the present experiment, acts to shake the position of the shear layer separated off the upstream corners over the distances comparable to this scale. When it shifts towards the surface, it can reach the surface resulting in the flow reattachment. This was indicated by the local reduction of the surface pressure and its propagation in the downstream direction. This was seen to occur intermittently at a frequency higher than the vortex shedding. The periodicity of this motion is weak but shows as a mild peak at the low end of broad spectrum representing turbulent fluctuations. Though it may be confused as a secondary shedding frequency it is better interpreted as the contributions from the large-scale turbulent motion.

5
Conclusions

The present paper presents new and detailed statistics of aerodynamic pressure and forces on rectangular cylinders of various length-to-height ratios in smooth and turbulent streams. The instantaneous and simultaneous measurements of surface pressure at multiple positions on the cylinder surface allowed documentation of instantaneous and fixed-phase distributions of fluctuating pressure as well as other long-time statistics such as spectra and correlations. These clarify much of the effects of the free-stream turbulence and also provide a comprehensive test case for validation of simulation methods.

The turbulence generated in the inflow is very close to isotropic, with spectra and coherence following approximately the Kármán spectrum and Davenport coherence with the length scale of the same order as the cylinder height. The results may be interpreted as the effects of uniform isotropic turbulence.

The main effects are seen when B/D is in the critical range near B/D=2.5. The turbulence in the inflow with the length scale of the same order as D acts to move the po-

本論文は，Experiments in Fluids 34, 2003 より転載したものである。

sition of the shear layer separated off the upstream corners, and this is the main mechanism for promoting reattachment. When the reattachment occurs, the vortex shedding is weakened significantly or suppressed. At the same time, the spanwise correlation of fluctuating pressure on the side surfaces is reduced, while that on the rear surface increases.

References

Bearman PW, Obasaju ED (1982) An experimental study of pressure fluctuation on fixed and oscillating square-section cylinder. J Fluid Mech 119:297–321

Bearman PW, Trueman DM (1972) An investigation of the flow around rectangular cylinders. Aeronaut Q 23:229–237

Durao DFG, Heitor MV, Pereira JCF (1988) Measurement of turbulent and periodic flows around a square cross-section cylinder. Exp Fluids 6:298–304

Ishizaki I, Katsura J (1974) On the distribution of pressure-fluctuation correlation on the side surface of two-dimensional models with slender rectangular cross sections. J Struct Constr Eng, AIJ 220:29–34 (in Japanese)

Lee BE (1975a) The effects of turbulence on the surface pressure field of a square prism. J Fluid Mech 69:263–282

Lee BE (1975b) Some effects of turbulence scale on the forces on a bluff body. J Ind Aerodynamics 1:361–370

Lyn DA, Rodi W (1994) The flapping shear layer formed by flow separation from the forward corner of a square cylinder. J Fluid Mech 264:353–376

Miyazaki M, Miyata T, Ito M (1980) Characteristics of steady and unsteady pressure distributions around a rectangular cylinder in turbulent flow. In: Proceedings of the 6th Symposium on Wind Engineering. Japan Association for Wind Engineering, Tokyo, pp177–184 (in Japanese)

Mizota T, Okajima A (1982) On the separated flow and variation of fluid force around a rectangular cylinder with section ratio 0.4 to 1.5 in a uniform flow. In: Proceedings of the 7th Symposium on Wind Engineering. Japan Association for Wind Engineering, Tokyo, pp 75–81(in Japanese)

Nakaguchi H, Hashimoto T, Takefuji M (1968) Experiments on drag on cylinders of rectangular cross section. Aeronaut Space Sci Jpn 16:1–5

Nakamura Y, Ohya Y (1984) The effects of turbulence on the mean flow past two-dimensional rectangular cylinders. J Fluid Mech 149:255–273

Okajima A (1982) Flow around cylinders of rectangular cross sections with various length to height ratios. J Wind Eng 17:75–81

Ootsuki S, Fujii K, Washizu H, Ohya S (1980) On the characteristics of three-component aerodynamic force and pressure distribution of a fixed two-dimensional recrtangular cylinder in a uniform flow. In: Proceedings of the 6th Symposium on Wing Engineering, Japan Association for Wind Engineering, Tokyo, pp153–159 (in Japanese)

Petty DG (1979) The effects of turbulence intensity and scale on the flow past square prisms. J Ind Aerodyn 3:247–252

Roberson JA, Lin CY, Rutherford GS, Stine MD (1972) Turbulence effects on drag of sharp-edged bodies. ASCE J Hydraul Division HY7:187–1203

Tamura T, Miyagi T (1988) The effects of corner shape on aerodynamic characteristics of square cylinder. J Struct Construct Eng, AIJ, No. 514:51–58 (in Japanese)

Vickery BJ (1966) Fluctuating lift and drag on a long cylinder of square cross-section in a smooth and in a turbulent stream. J Fluid Mech 25:481–494

Yoshida M, Hongo T, Suzuki M, Ookuma T, Marukawa H (1986) Frequency characteristics of fluctuating pressure in lead tubes. In: Proceedings of the 11th Symposium on Wind Engineering. Japan Association for Wind Engineering, Tokyo, pp 75–81 (in Japanese)

本論文は，Experiments in Fluids 34, 2003 より転載したものである。